RSC Pharmaceutics

ROYAL SOCIETY OF CHEMISTRY

PAPER

View Article Online
View Journal | View Issue

Cite this: *RSC Pharm.*, 2025, **2**, 1533

Exploring hot melt extrusion in the formation of exemestane/amino acid co-amorphous systems

Ioannis Partheniadis, Maria Tsouka and Ioannis Nikolakakis *

Co-amorphous systems (CAMS) of exemestane (EXE) were prepared with three amino acid (AA) co-formers of increasing hydrophobicity: (i) L-lysine (LYS), (ii) L-valine (VAL) and (iii) L-methionine (MET) using feed solvent pretreatment hot-melt extrusion (mHME). Thermal analysis (DSC and TGA) guided processing parameters confirmed the class III glass-forming ability of EXE (T_g = 91.2 °C). Hansen solubility parameters ($\Delta\delta_t$ < 4 $MPa^{1/2}$) predicted favorable drug/co-former miscibility. PXRD and DSC demonstrated successful co-amorphization for molar ratios of EXE/LYS (1 : 1 and 1 : 2), EXE/MET (1 : 1) and EXE/VAL (2 : 1 drug/AA). ATR-FTIR indicated co-amorphization predominantly by simple molecular mixing with only weak interactions. The physical stability of CAMS was evaluated by isothermal microcalorimetry, dynamic mechanical analysis (DMA) and crystallographic profiles (pXRD) obtained at different times during accelerated stability tests (40 °C, 75% RH). EXE/LYS systems exhibited the longest relaxation times (τ_D^β), translating as excellent physical stability, which corroborated the results of accelerated tests. EXE/MET showed moderate stabilization, while EXE/VAL was the least stable. Under non-sink conditions of the dissolution test, EXE/LYS (1 : 1) presented a pronounced spring–parachute profile with sustained supersaturation, outperforming other EXE/AA CAMS.

Received 27th May 2025,
Accepted 24th August 2025

DOI: 10.1039/d5pm00146c

rsc.li/RSCPharma

Introduction

Co-amorphous systems (CAMS) have emerged as a technology to address the low bioavailability of modern drug candidates caused by their poor water solubility, limiting absorption.[1–4] By stabilizing the drug in its amorphous form, these systems enhance apparent solubility and drastically improve dissolution performance.

Unlike traditional approaches, CAMS utilize small organic molecules (co-formers) instead of polymers, enabling higher drug concentrations while avoiding moisture sorption problems associated with polymers' hygroscopicity.[5] Amino acids (AAs) are frequently employed as co-formers in CAMS.[2] To address the low thermal stability of AAs,[6] ball milling – which induces crystal defects to achieve amorphization – has been used for preparing such systems. However, ball milling faces challenges such as solvent dependency, scalability constraints, and industrial applicability due to limitations in the size of the equipment.[2,7–9]

Hot-melt extrusion (HME), a solvent-free, scalable process widely used for amorphous solid dispersions,[3,10–12] offers an alternative to prepare CAMS by thermomechanically disrupting the crystalline structure. To address the thermal instability of amino acids (AAs) and enable the processing of drug/AA CAMS, we previously developed a feed solvent pretreatment hot melt extrusion (mHME) method.[13,14] In this approach, diluted acetic acid was used to convert drug/AA powder mixtures into extrudable granular feed, enabling extrusion at lower temperatures, thus mitigating thermal degradation risks. Importantly, the CAMS produced by mHME had significantly improved drug solubility and release compared to the crystalline drug.

In a recent study, we prepared CAMS of griseofulvin (GRI) with three AAs differing in hydrophobicity using the mHME method.[14] While previous attempts to prepare GRI/AA CAMS using purely mechanical methods were only moderately successful,[15] the mHME method produced CAMS at different drug/AA molar ratios. Therefore, the mHME method presents an excellent alternative for the preparation of drug/AA CAMS where mechanical or purely thermal methods fail.

In the present study, we applied the mHME process for the development of CAMS of the poorly water-soluble drug exemestane (EXE) with three amino acids of different hydrophobicity and molecular side chains as co-formers: L-lysine (polar, positively charged), L-valine (hydrophobic, small aliphatic chain) and L-methionine (more hydrophobic, large aliphatic chain). Since in our previous work,[14] we had shown that griseofulvin with 6 hydrogen bond acceptor groups forms stable CAMS with L-lysine, L-methionine and L-valine and with improved

Department of Pharmaceutical Technology, School of Pharmacy, Faculty of Health Sciences, Aristotle University of Thessaloniki, 54124 Thessaloniki, Greece.
E-mail: yannikos@pharm.auth.gr; Tel: +302310997635

drug release, in the present work, we wanted to see to what extent this is possible with a drug of lower H-bonding potential such as exemestane (only 2 hydrogen bond acceptor groups). As in our previous publications,[13,14] CAMS were prepared using only drugs and amino acids without polymers. The produced CAMS were examined based on three critical attributes: co-formability, physical stability, and dissolution performance.[2]

Experimental

Materials

Exemestane (EXE; M_w = 296.40 g mol^{-1}) was chosen as a poorly water-soluble drug and L-lysine (LYS; M_w = 146.19 g mol^{-1}), L-methionine (MET; M_w = 149.21 g mol^{-1}) and L-valine (VAL; M_w = 117.25 g mol^{-1}) as the amino acid (AA) co-formers for CAMS. 30% w/w aqueous acetic acid solution (AcOH; CAS No. 64-19-7, Sigma-Aldrich Inc., Saint Louis, MO, U.S.A) was the feed pretreatment solvent.

Pretreatment of EXE/AA powder mixtures for hot melt extrusion processing

Drug/AA powder mixtures at 2 : 1, 1 : 1 and 1 : 2 molar ratios were prepared and 30% aqueous acetic acid (AcOH) solution (9 to 12 mL g^{-1}) was added. The AcOH solution was selected because it enabled the formation of a paste-consistency mass, resulting in granules after drying/sieving. This was subsequently dried in an air circulation oven (Heraeus, Germany) at 100 °C for 3 h, followed by sieving (850 μm sieve) to give a granular feed that was added to the extruder. More details on the feed pretreatment process are given elsewhere.[13,14]

Hot melt extrusion with feed solvent pretreatment (HME)

The extruder was a bench-type vertical single-screw (Model RCP-0250 Microtruder, Randcastle Extrusion Systems, NJ, USA) fitted with a 2 mm orifice die, operated at 20 rpm screw speed. Feeds were processed at extrusion zone temperatures ranging from 145 to 150 °C in the feeding zone, 165 to 175 °C in the mixing/melting/shearing/compression zone, and 170 to 185 °C in the extrusion zone. More details about the preparation method are given elsewhere.[13] Extrudate codes, drug/AA molar ratios of the nine extruded feeds (three amino acids at three EXE/AA molar ratios), together with % drug content in the extrudates determined by high liquid pressure chromatography, are listed in Table 1. The zone temperatures applied for the extrusion of the nine EXE/AA feeds together with the decomposition temperatures (T_{dec}) of the feeds measured by thermogravimetry (TGA) are given in Table 2.

Differential scanning calorimetry (DSC)

Formation of CAMS from the drug/AA powder mixtures was studied *in situ* using the DSC204 F1 Phoenix DSC instrument (NETZSCH, Germany). Accurately weighed samples of 3–4 mg were placed in pierced aluminum pans and examined for thermal changes at 10 °C min^{-1} heating rate under nitrogen gas. Indium was used for instrument calibration. Additionally, DSC was applied to determine the glass forming ability (GFA) of EXE, based on the classification system for crystallization tendency proposed by Baird *et al.*[16] A 1st heating cycle was applied to erase thermal history, followed by fast cooling (at 20 °C min^{-1}) and a 2nd heating cycle to estimate the GFA.

In certain cases, modulated DSC (mDSC) was applied to confirm the presence of a single glass transition temperature (T_g). For this measurement, the sample (10–15 mg) was equilibrated at 30 °C for 2 min before ramping at 2 °C min^{-1} up to 180 °C using a modulation of ±0.212 °C every 40 s. A reverse sample heat flow was processed using the Proteus Analysis® software to confirm the single T_g.

Thermogravimetric analysis (TGA)

The thermal stability of ingredients and drug/AA mixtures was examined over a wide temperature range using a TGA instrument connected to a TA-60-WS controller (Shimadzu Corporation, Kyoto, Japan). Safe HME processing temperature ranges were established to avoid overheating and decomposition during extrusion. For the analysis, 3–4 mg of accurately weighed samples were placed in aluminum pans and heated

Table 1 Codes and compositions as molar ratios and weight content (%) of the nine drug/amino acid mixture feeds that were processed by hot-melt extrusion, and drug content analyzed in the extrudates by high pressure liquid chromatography

Code	Amino acid (AA)	Molar ratio		Composition (% w/w) of the feed		Drug content (% w/w)
		Drug	AA	Drug	AA	
EXE/LYS 2 : 1	L-Lysine	2	1	80.25	19.75	98.8 ± 0.3
EXE/LYS 1 : 1		1	1	67.00	33.00	97.9 ± 0.4
EXE/LYS 1 : 2		1	2	50.25	49.75	98.7 ± 0.3
EXE/MET 2 : 1	L-Methionine	2	1	80.00	20.00	99.3 ± 0.6
EXE/MET 1 : 1		1	1	66.50	33.50	99.0 ± 0.2
EXE/MET 1 : 2		1	2	49.75	50.25	98.9 ± 0.4
EXE/VAL 2 : 1	L-Valine	2	1	83.50	16.50	99.1 ± 0.3
EXE/VAL 1 : 1		1	1	71.50	28.50	98.6 ± 0.2
EXE/VAL 1 : 2		1	2	55.75	44.25	99.4 ± 0.1

Table 2 Extrusion zone temperatures applied during the hot-melt extrusion of the nine experimental drug/AA molar ratios (physical mixtures) together with their decomposition temperatures

Drug/AA molar ratio	Temperature zones (°C)			Decomposition temp. (T_{dec} °C)	Difference T_{dec} − T3 (zone 3)
	T1	T2	T3		
EXE/LYS 2 : 1	150	165	170	193.3	23.3
EXE/LYS 1 : 1	150	165	170	195.6	25.6
EXE/LYS 1 : 2	150	165	170	196.8	26.8
EXE/MET 2 : 1	145	170	180	199.9	19.9
EXE/MET 1 : 1	145	175	185	201.3	16.3
EXE/MET 1 : 2	145	175	185	203.8	18.8
EXE/VAL 2 : 1	145	170	180	197.8	17.8
EXE/VAL 1 : 1	145	170	180	198.2	18.2
EXE/VAL 1 : 2	145	170	185	200.3	15.3

under a nitrogen atmosphere (N_2) at 10 °C min^{-1}. Degradation temperature was determined from the onset temperature according to American Standard Test Method (ASTM E2550)[17] specifications. Experiments were conducted in triplicate.

Drug/AA miscibility from Hansen solubility parameters (HSPs)

Hansen solubility parameters (HSPs) were computed as a thermodynamic guide to the miscibility of the drug and AA co-formers. It is a simple, direct method to predict miscibility of components and provides a reliable prediction of CAMS formation and physical stability.[13,14] The total Hansen solubility parameter (δ_t) represents attractive intermolecular forces and can be expressed as the square root of the sum of dispersion, polar and hydrogen bonding parameters (HSPs). A difference of $\Delta\delta_t < 5$ $MPa^{1/2}$ is a criterion of miscibility.[18–20] HSPs for the drugs and AAs were calculated according to the group contribution method previously described.[21]

Quantification of the drug in the extrudates

Quantification of exemestane (EXE) was undertaken using high pressure liquid chromatography (HPLC). The HPLC system consisted of a pump (LC-10 AD VP), an auto-sampler (SIL-20A HT), and a UV-Vis detector (SPD-10A VP, Shimadzu, Kyoto, Japan). The analytical conditions were adapted from the literature with slight modifications.[22] The mobile phase comprised acetonitrile (ACN) and water in a ratio of 50 : 50 v/v. The stationary phase was a Discovery H C18 column (150 mm, 4.6 mm, 5 μm, Merck KGaA, Darmstadt, Germany) and the flow rate was set to 1.0 mL min^{-1}, with an injection volume of 10 μL. The detection wavelength was 242 nm. The mobile phase was degassed under vacuum (20 min) and sonicated (10 min) before each analysis. Standard samples of the API were analyzed, with concentrations in the range of 9.0–900.0 μg mL^{-1} ($R^2 \geq 0.999$).

Attenuated total reflectance Fourier transform infrared spectroscopy (ATR-FTIR)

Spectra of the samples were acquired using a Bomem FTIR spectrometer (MB-Series, ABB Bomem Inc., Quebec, QC, Canada) and processed by GRAMS/AI software (version 7.0, Thermo Fisher Scientific, Waltham, MA, USA). The samples were scanned over a wavenumber range from 400 to 4000 cm^{-1} with a resolution of 4 cm^{-1}. The spectra were averaged from 64 scans.

Powder X-ray diffraction (pXRD) of extrudates after preparation and during stability testing

To estimate the crystalline and by difference the amorphous content of unprocessed ingredients, feeds and extruded products, pXRD was applied. 1 g of sample was gently pulverized using a porcelain mortar, and then it was mounted on a 28-position sample plate and analyzed using transmission pXRD (λ = 0.15405 nm, CuKα radiation, Bruker D8 PHASER CRD-diffractometer, Bruker, MA, USA). Data were collected in the range of 5–35° 2θ at 0.02° 2θ step size and 0.5 s step count time. Instrument accuracy was tested against a corundum A26-B29-S reference sample.

For the solid-state stability of CAMS in the extrudates, pXRD analysis was applied. The samples were placed in desiccators at 45 °C and 75% RH. To detect and quantify any solid-state changes, pXRD profiles were obtained at day 0, 30 and 90 days, analyzed and compared.

Isothermal microcalorimetry relaxation measurements using a thermal activity monitor

A thermal activity monitor (TAM III, TA Instruments, New Castle, USA) was used to directly measure the relaxation time of amorphous samples by recording the rate of enthalpy relaxation as a function of time during annealing.[23] Samples of approximately 200 mg were prepared in 4 mL disposable crimp-sealed ampoules and measured at 25 °C. To minimize the effect of thermal history, freshly prepared samples were collected and loaded into the equilibrium position. The resulting power–time curves were fitted to the derivative of the 'Modified Stretched Exponential' (MSE) equation (eqn (1)) to obtain the parameters τ_0, τ_1, and β.[24,25]

$$P = 277.8\frac{\Delta H_r(\infty)}{\tau_0}\left(1+\frac{\beta t}{\tau_1}\right) \times \left(1+\frac{t}{\tau_1}\right)^{\beta-2} \exp\left[-\left(\frac{t}{\tau_0}\right)\left(1+\frac{t}{\tau_1}\right)^{\beta-1}\right] \quad (1)$$

In eqn (1), P is the power (μW g^{-1}), and t is the measurement (annealing) time (h). The number 277.8 accounts for unit conversions. τ_0 and τ_1 are relaxation time constants, β represents the distribution of independently relaxing states ($0 < \beta < 1$) and $\Delta H_r(\infty)$ is the relaxation enthalpy at infinite time obtained from eqn (2):

$$\Delta H_r(\infty) = (T_g - T) \times \Delta C_p \quad (2)$$

T_g is the glass transition temperature, ΔC_p is the heat capacity change at T_g, and T is the annealing temperature. The relaxation time (τ_D^β) can then be calculated from eqn (3):

$$\tau_D^\beta = \left(\tau_0^{\frac{1}{\beta}} \times \tau_1^{\frac{\beta-1}{\beta}}\right)^\beta \quad (3)$$

Statistical analyses and fitting of the experimental data to the MSE equation were conducted using Python (version 3.11.7) and the SciPy optimization module (scipy.optimize, version 1.14.1), and Jupyter Notebook IDE (version 7.0.8).

Apparent equilibrium solubility of drugs in aqueous solutions

The apparent equilibrium solubility of EXE was determined both in the crystalline and amorphous drug forms (prepared by quench-cooling) and the corresponding methods are described below separately for each drug form.

Crystalline drug form. Excess amounts were added in small vials containing 30 mL of deionized water (pH 5.5). The vials were vortexed for 20 s and subsequently placed for 72 h in a horizontally shaking water bath (25 °C, WBS-30, Witeg

Labortechnik GmbH, Wertheim, Germany) under agitation. Aliquots were withdrawn, filtered (0.45 μm, Sigma-Aldrich Inc., Saint Louis, MO, U.S.A) and analyzed by HPLC as described above (n = 6). The equilibrium solubility, C_s, of crystalline EXE in water was 31.5 ± 2.9 μg mL^{-1}.

Amorphous drug. The UV-extinction method was applied for the determination of the equilibrium solubility of the amorphous drug, based on previously reported studies.[26–28] This method determines indirectly the amorphous solubility (not a true thermodynamic term) based on the onset of the liquid–liquid phase separation (LLPS). 15 mL of deionized water (pH 5.5) was placed in a Falcon tube, which was immersed in a beaker and kept at 37 ± 0.5. A 10 mg mL^{-1} drug solution in ethanol was added to deionized water at 5 μL volume increments and the UV-Vis spectrum (400–600 nm) was recorded after each 5 μL addition. The concentration at which an increase in absorption was observed was taken as the amorphous solubility of the drug. It was found to be 42.1 ± 1.3 μg mL^{-1}.

Precipitation study to evaluate the association tendency of EXE with AAs in solution

To elucidate the re-crystallization tendency of EXE from the CAMS during *in vitro* dissolution, the impact of amino acids (AAs) on the potential depletion and precipitation of EXE from a pre-supersaturated drug solution was studied by applying the Solvent Shift method.[29] Tests were conducted in triplicate on a USP II apparatus (rotating paddle, Pharma Test PTW 2, Hainburg, Germany) at 37 ± 0.5 °C and 50 rpm paddle rotation speed. First, EXE was solubilized in a small volume of dimethyl sulfoxide (100 mg EXE in 20 mL DMSO). This solution was added to 450 mL solution of each AA in deionized water (DMSO and water are miscible), aiming for a sink index (SI) of 0.116 (*i.e.* 245 mg of EXE in 900 mL of aqueous medium), where SI = crystalline drug solubility over the concentration of completely dissolved drug.[29] The amount of each AA pre-dissolved in the deionized water corresponded to a 1 : 1 EXE/AA molar ratio in the final combined solution, which was found to be the optimal ratio for CAMS formation. Aliquots were collected over a 120 min time period, filtered through PVDF filters (0.45 μm) and analyzed by HPLC as described in the experimental part.

In vitro dissolution tests

Due to the expected higher solubility of the amorphous drug from the CAMS, the tests were conducted under non-sink conditions using a USP II apparatus (rotating paddle, Pharma Test PTW 2, Hainburg, Germany) at 37 ± 0.5 °C and 50 rpm paddle rotation speed. Samples of extrudates containing 1220 mg of drug each were added to 450 mL of deionized water (SI = 0.0116). Before the test, the medium was degassed to avoid powder floating. 2.5 mL aliquots were automatically withdrawn for analysis and immediately replaced with fresh dissolution medium with the aid of a motorized sampling system consisting of a fraction collector (PTFC-2/8 SP, Pharma Test, Hainburg, Germany) and two syringe pumps (PT-SP6, Pharma Test, Hainburg, Germany). The aliquots were filtered (0.45 μm, PVDF filters) and analyzed by HPLC as described previously. At the end of the test, the precipitants were filtered using a Buchner funnel under vacuum, dried at room temperature for 12 h and analyzed for crystallinity by pXRD (n = 3).

Results and discussion

Hot melt extrusion – thermal analysis and processing temperatures

Fig. 1 presents the DSC and TGA thermographs of neat EXE and AA powders. Thermographs of drug/AA crystalline powder mixtures at 2 : 1, 1 : 1 and 1 : 2 molar ratios are presented in Fig. S1 (SI). EXE melts at 198.9 °C (ΔH_f = 93.4 J g^{-1}) and decomposes above 205.6 °C (Fig. 1(a)). From the AAs, LYS shows T_m at 204.4 °C (ΔH_f = 177.4 J g^{-1}) and T_{dec} above 173.4 °C with 2.8% weight loss at T_m (Fig. 1(c)), MET shows T_m at 291.5 °C (ΔH_f = 908.6 J g^{-1}) and T_{dec} above 267.8 °C with 2.5% weight loss at T_m (Fig. 1(d)) and VAL shows T_m at 301.2 °C (ΔH_f = 863.4 J g^{-1}) and T_{dec} above 281.5 °C with 1.7% weight loss at T_m (Fig. 1(e)). Fig. S1 presents DSC thermograms of the physical drug/amino acid mixtures. Thermograms taken with sealed pans gave the same melting temperatures as with pierced pans but also multi-peaks near T_{dec} due to entrapped decomposition compounds.

Besides the thermal events of individual components, the decomposition temperatures (T_{dec}) of the drug/AA physical mixtures were determined (Fig. S1). These were used as a guide for the choice of hot-melt extrusion to ensure safe operation below the T_{dec}, since they were different from the single component T_{dec}. Accordingly, the TGA weight-loss profiles alongside DSC decomposition peaks were recorded (Fig. 1 and Fig. S1), and the T_{dec} values are listed in Table 2. They range from 193.3 °C to 203.8 °C, depending on the EXE/AA ratio. By comparing these values with extrusion temperatures (Table 2, highest in zone 3), there is a safety margin of 15.3 °C to 26.8 °C, suggesting low degradation risk. Highest margins (23.3–26.8 °C) are seen for the EXE/LYS combinations. This safety margin is attributed to the feed solvent pretreatment, which imparted plasticization to the mass and reduced extrusion temperatures compared to temperatures needed to extrude the physical mixtures.[13]

Analysis of the drug content in the extruded products

To confirm that no drug decomposition occurred during extrusion, the extrudates were analyzed by HPLC and the results are presented in Table 1 (last column). The recovered drug ranged from 97.9 to 99.4% w/w of that added in the feeds, indicating negligible loss. Although the coexistence of the drug with AA may decrease the melting temperature and T_{dec} of EXE, the great reduction in the required extrusion temperatures due to feed pretreatment more than compensates for any T_{dec} decrease of the drug due to pretreatment.

Evaluation of CAMS

The evaluation of the developed CAMS was based on three critical quality attributes (CQAs): (i) co-formability, (ii) physical stability, and (iii) dissolution performance.[2]

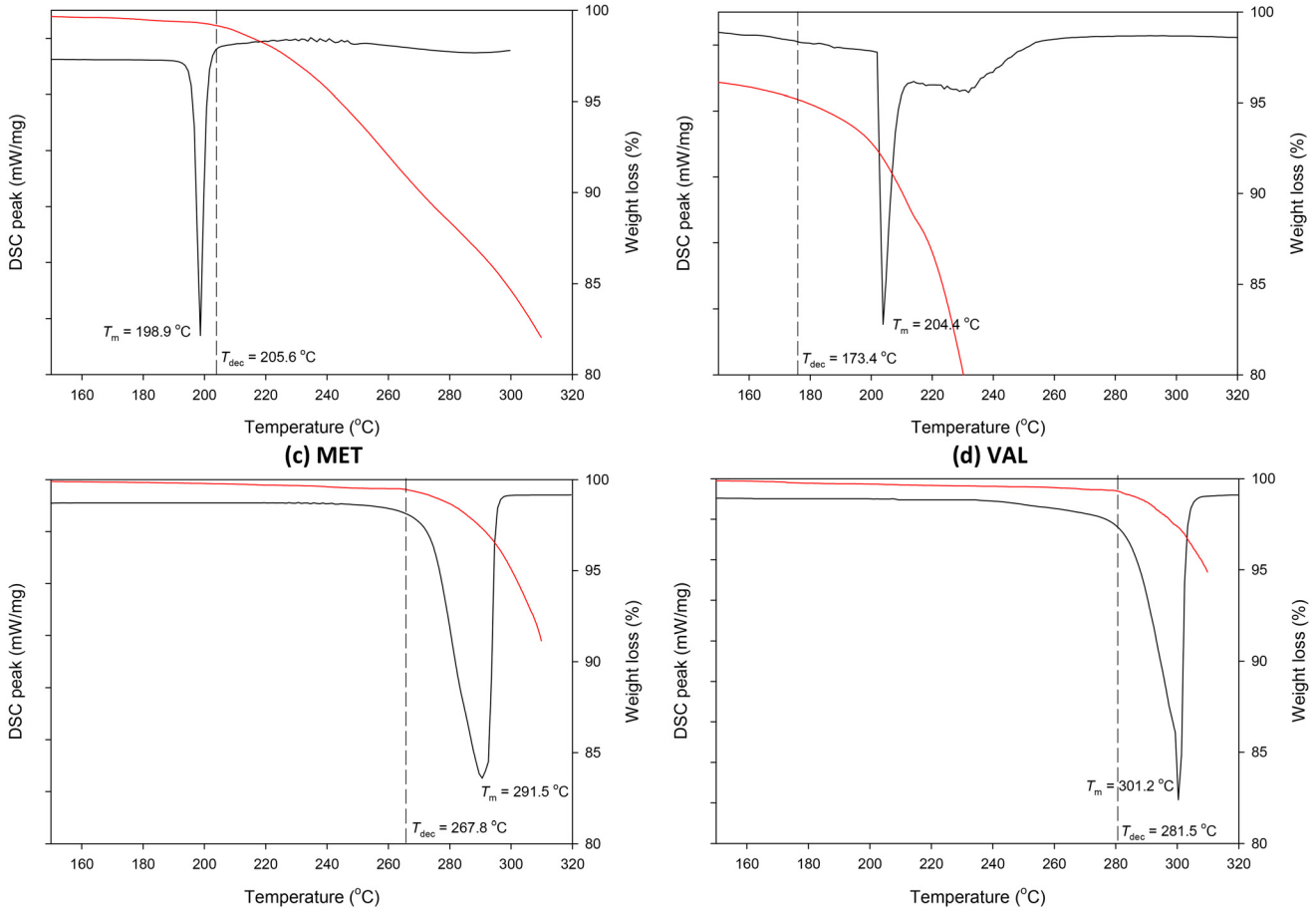

Fig. 1 DSC and TGA thermographs for unprocessed materials: (a) exemestane (EXE), (b) L-lysine (LYS), (c) L-methionine (MET) and (d) L-valine (VAL).

Co-formability of the amino acids with the drug. Co-formability refers to the selection of the appropriate co-former for the drug to achieve co-amorphization.

Glass-forming ability of drugs. In Fig. 2, DSC thermograms of EXE obtained during heating–cooling–reheating cycles are presented. In the 1st heating cycle, the drug shows a melting endotherm (T_m) at 198.9 °C. No recrystallization peaks are observed upon cooling. In the 2nd heating cycle, T_g is observed at 91.2 °C. Therefore, EXE can be characterized as a class III glass former.[16]

Thermodynamic miscibility. The Hansen solubility parameters of the selected AAs and EXE were computed to predict miscibility and the possibility of drug/AA CAMS formation. In Table 3, Hansen solubility parameters together with the number of H-bond acceptor and donor groups for each molecule are presented. It can be seen that in all cases, the total solubility parameter difference ($\Delta\delta_t$) between the drug and each AA is well below 4 $MPa^{1/2}$, indicating good miscibility and a strong possibility for CAMS formation.[18–20]

Solid-state characterization of extrudates by pXRD. In Fig. 3, pXRD patterns of crystalline (cEXE) and amorphous (aEXE) drugs and of crystalline AA (cLYS, cMET and cVAL) powders are presented. cEXE reflections appear at 10.8°, 14.5°, 15.9°, 16.8°, 18.1°, 19.7°, 21.5°, 22.7°, 23.4°, 24.4°, 26.2°, and 29.2° 2θ.[30] In the pXRD patterns of the AAs, the following strong reflections are observed: for cLYS at 5.1°, 10.8°, 17.6°, 24.5°, 31.4°, and

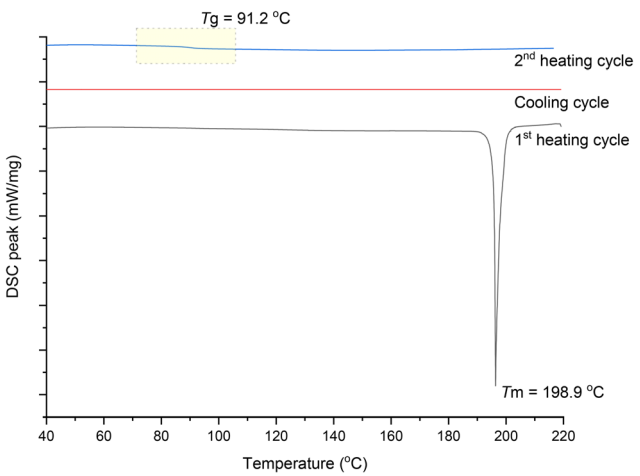

Fig. 2 DSC thermograms of exemestane during the heating (1st cycle, black)–cooling (red)–heating (2nd cycle, blue) cycle for the determination of its glass forming ability.

Table 3 Computed Hansen solubility parameters (MPa)$^{1/2}$

Material	δ_d	δ_p	δ_{hb}	δ_t	$\Delta\delta_t$	H-bond acceptor/donor
Exemestane	19.3	6.5	0.2	20.4	—	2/0
Lysine	16.9	6.0	10.9	21.0	0.6	4/3
Methionine	17.4	13.2	10.2	24.1	3.7	4/2
Valine	18.9	13.0	7.7	24.2	3.8	3/2

δ_d – dispersion forces; δ_p – polar forces; δ_{hb} – hydrogen-bonding attraction. δ_t – total solubility, representing all intermolecular attractive forces.

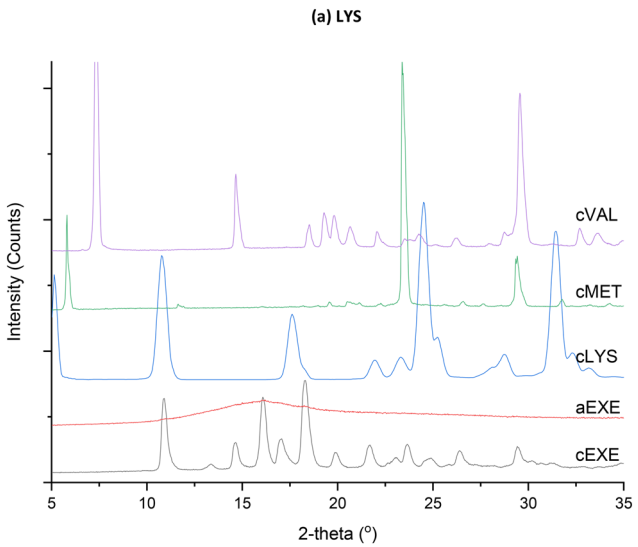

Fig. 3 pXRD patterns of unprocessed crystalline (cEXE) and amorphous (aEXE) exemestane prepared by quench cooling, and of unprocessed crystalline amino acids: L-lysine (cLYS), L-methionine (cMET), and L-valine (cVAL).

38.4°2θ; for cMET at 5.7°, 23.1°, 29.0°, and 35.1° 2θ; and for cVAL at 7.3°, 14.6°, 21.9°, 29.4°, and 39.9° 2θ.[31,32] Therefore, all unprocessed materials (drug and AAs) were crystalline. On the other hand, quench cooling successfully amorphized the drug (aEXE), since its pXRD pattern only shows a halo but no crystalline reflection peaks.

In Fig. 4, pXRD patterns of drug extrudates with the three AAs are presented. Co-amorphization was not achieved for all molar ratios examined. EXE formed CAMS with LYS at drug/AA molar ratios of 1 : 2 and 1 : 1, with MET forming CAMS only at a ratio of 1 : 1 and with VAL only at 2 : 1. CAMS can be produced at various molar ratios, not just equimolar. Stoichiometry plays an important role in the formation of CAMS, with more than 70% of the reported CAMS prepared at equimolar ratios and 23.1% of the CAMS prepared at other molar ratios.[2] This has also been found in our previous studies.[13,14] Although co-amorphization was not quantitatively assessed, visual inspection of the pXRD patterns (Fig. 4) suggests that among the different drug/amino acid combinations, EXE/LYS exhibits the highest degree of amorphization. This is indicated by the absence of pronounced diffraction peaks in the pXRD patterns of EXE/LYS compared to EXE/MET and EXE/VAL, and it is attributed to the lower $\Delta\delta_t$ values (Table 3), implying better miscibility.

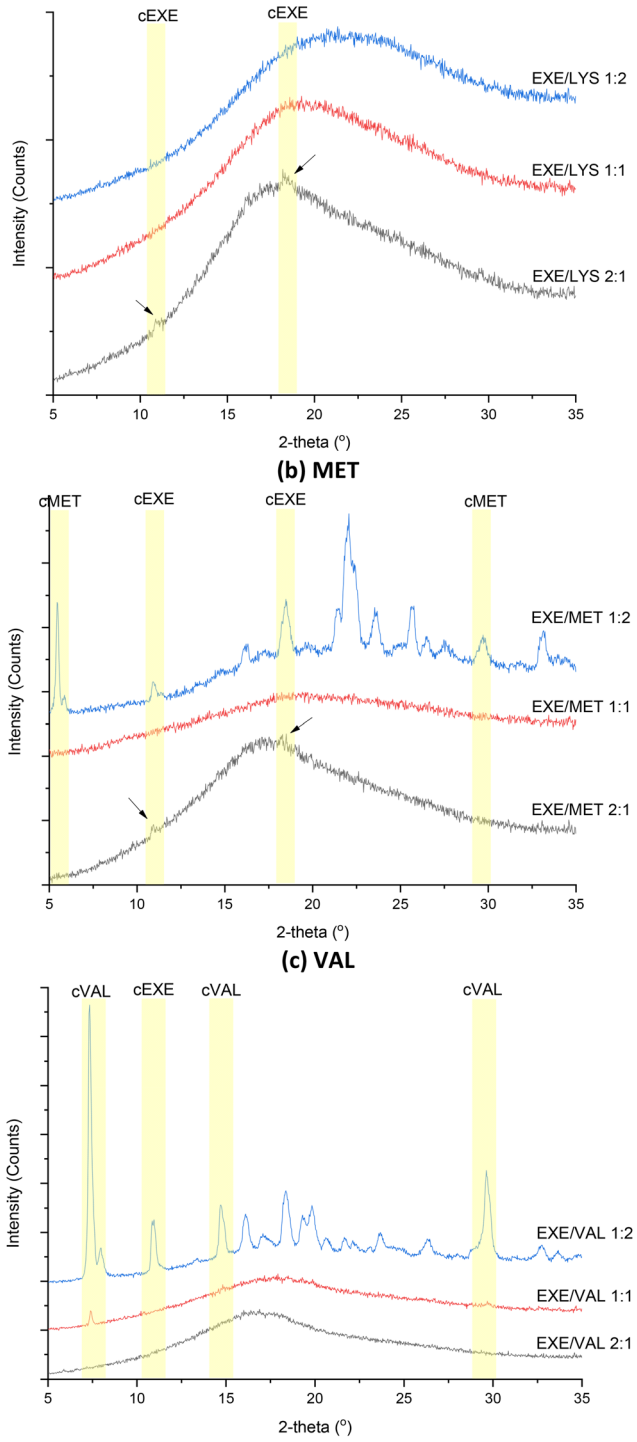

Fig. 4 pXRD patterns of exemestane extruded products with (a) L-lysine (LYS), (b) L-methionine (MET), and (c) L-valine (VAL).

Molecular interactions. Fig. 5 presents ATR-FTIR spectra of the crystalline drug (cEXE), AA crystalline powders (cLYS, cMET and cVAL) and amorphous drug (aEXE). The spectrum

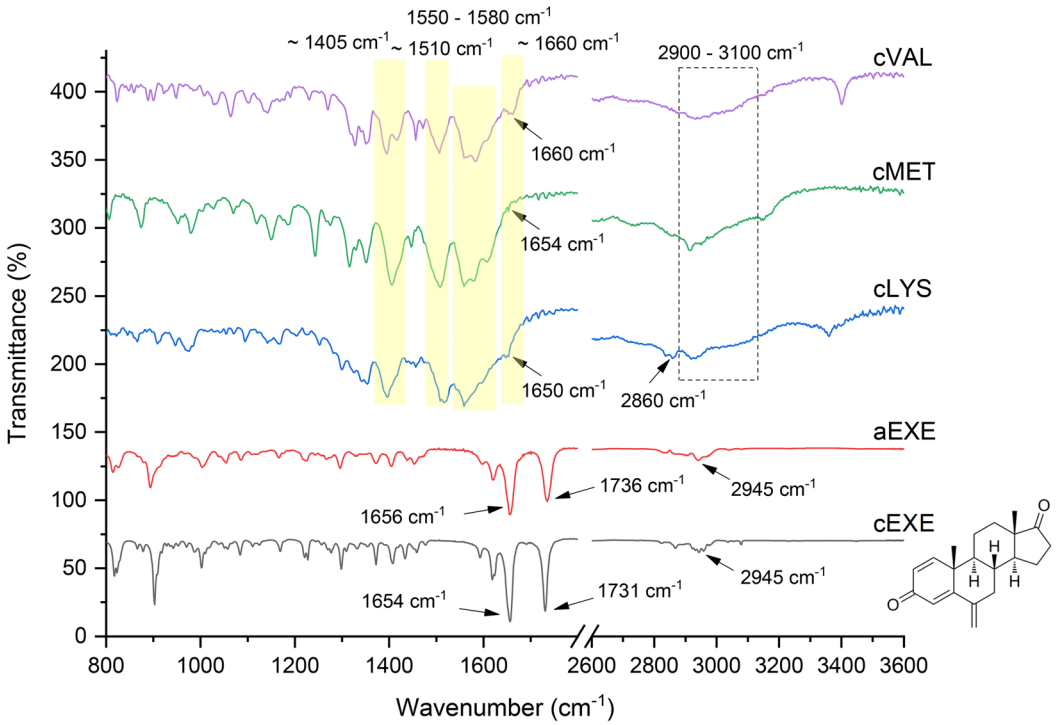

Fig. 5 ATR-GTIR spectra of crystalline (cEXE) and amorphous exemestane (aEXE) and of unprocessed crystalline: L-lysine (cLYS), L-methionine (cMET), and L-valine (cVAL) (chemical structure of EXE is shown on the side).

of cEXE shows the characteristic drug peaks with stretching vibrations of the $-CH_2-$ group at 2937 cm^{-1}, of the cyclopentene ring (D ring) –C═O group at 1730 cm^{-1}, of the cyclohexadiene ring (A ring) –C═O group at 1654 cm^{-1} and of the –C═C– group at 1620 cm^{-1}.[33] The aEXE spectrum shows minor changes compared to cEXE, associated with structural rearrangements. More specifically, there is a shifting of the two –C═O groups to higher wavenumbers, from 1730 to 1737 cm^{-1} and from 1654 to 1656 cm^{-1}, respectively.

The ATR-FTIR spectra of crystalline amino acids (cLYS, cMET, and cVAL; Fig. 5) show the characteristic peaks of AAs. The wide peak between 2900 and 3000 cm^{-1} due to the –OH stretching vibrations of the carboxylic group, the peaks at 1650 cm^{-1} for cLYS, 1652 cm^{-1} for cMET and 1660 cm^{-1} for cVAL due to the –NH bending vibrations of the amine group, the peaks between 1550 and 1580 cm^{-1} (1560 for cLYS, 1567 for cMET and 1574 for cVAL) due to –C═O stretching vibrations of the carboxylic group, and the peaks at *ca.* 1510 cm^{-1} (1514 for cLYS, 1508 for cMET and 1506 for cVAL) and *ca.* 1410 cm^{-1} (1400 for cLYS, 1405 for cMET and 1398 for CVAL) due to C–H stretching vibrations.[34,35] The small 2860 cm^{-1} peak in the spectrum of cLYS is due to the CH_2 asymmetric stretching vibrations.

Fig. 6 shows the ATR-FTIR spectra of EXE/AA extruded CAMS and corresponding physical mixtures of the studied molar ratios in the 1400–1800 cm^{-1} region of vibration of the two drug carbonyl groups. There are no significant changes between the spectra of extrudates and physical mixtures (PM). A small shift of the drug peak at 1731 cm^{-1} is seen for all CAMS spectra, and a drop in the intensities of the 1654 and 1731 cm^{-1} peaks for the EXE/LYS 1 : 2 and EXE/MET 1 : 1 CAMS. However, these differences should not be ascribed to molecular interactions. As already discussed, aEXE shows a small shift of this peak from 1731 to 1737 cm^{-1} (Fig. 5) compared to cEXE. Therefore, the EXE/AAs extruded CAMS are simply molecular drug/AA associations. The absence of drug/AA molecular interactions partly explains the unsuccessful co-amorphization of EXE/LYS 2 : 1, EXE/MET 1 : 2 and 2 : 1, and EXE/VAL 1 : 2 and 1 : 1 ratios, unlike the combinations of griseofulvin with the same AAs, which formed CAMS at all three molar ratios.[14]

Physical stability of successfully prepared CAMS. Physical stability studies were carried out for EXE/LYS 1 : 2 and 1 : 1, EXE/MET 1 : 1 and EXE/VAL 2 : 1 molar ratios, which produced CAMS.

Glass transition temperature. Fig. 7 presents modulated DSC (mDSC) thermograms of CAMS of EXE/AA LYS at ratios of 1 : 1 and 1 : 2, MET at a ratio of 1 : 1 and VAL at a ratio of 2 : 1, together with recorded glass transition temperatures (T_gs). A single T_g is seen in all cases, confirming the formation of homogeneous single-phase CAMS. The recorded T_gs (from 90.8 to 91.9 °C, Fig. 7) are close to that of amorphous EXE (91.2 °C, Fig. 2). An increase in the T_g of CAMS over the drug's T_g is generally associated with enhanced intermolecular forces and physical stability.[1,2] However, stable drug/AA CAMS have been prepared with T_g close to the drug, signifying that a

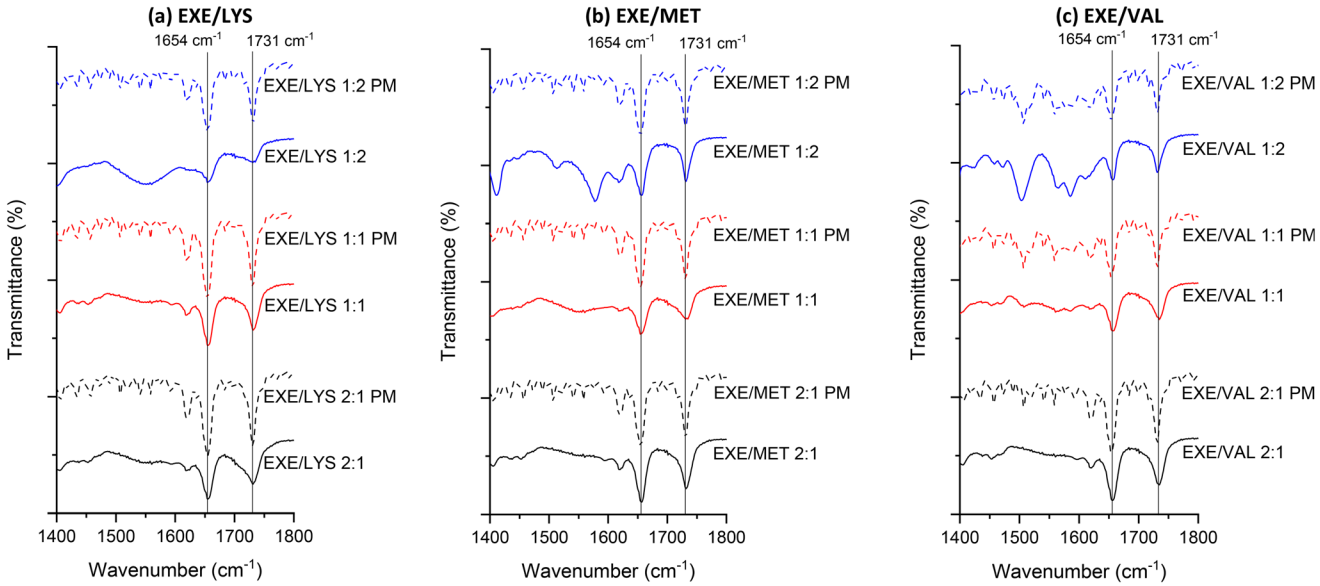

Fig. 6 ATR-FTIR spectra of exemestane/amino acid extruded products (solid lines) and the corresponding physical mixtures (PM) (dotted lines) with (a) L-lysine (EXE/LYS), (b) L-methionine (EXE/MET) and (c) L-valine (EXE/VAL) in the region of the vibrations of the two carbonyl drug groups (1400–1800 cm^{-1}).

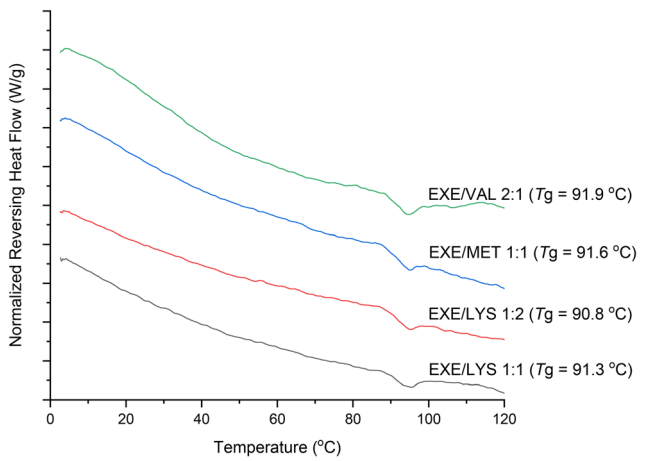

Fig. 7 Modulated DSC (mDSC) thermograms and recorded T_g values of CAMS of exemestane with L-lysine (EXE/LYS), L-methionine (EXE/MET) and L-valine (EXE/VAL) at molar ratios where CAMS were formed.

higher T_g of CAMS compared to the drug is not a prerequisite for stability.[13] This is supported by a number of studies, some of which are cited below. Adhikari *et al.*[35] used ceftazidime (T_g 48 °C) with tryptophan (T_g 128 °C) to form CAMS with T_g ~49 °C (Fig. S2 in their paper). Adhikari *et al.*[37] used ceftazidime (T_g 48 °C) with leucine (T_g theoretical 128 °C) to form CAMS with T_g ~50 °C. Kasten *et al.*[31] used binary drug/AA combinations of carvedilol (T_g 38 °C), furosemide (T_g 78 °C), indomethacin (T_g 45 °C), and mebendazole (T_g 110 °C) with MET, VAL, and LYS to form CAMS with T_gs close to those of the drugs (Fig. 1 in their paper). Liu *et al.*[2] used budenoside (T_g 89 °C) with arginine (T_g 55 °C) to form CAMS with T_gs between 89 and 93 °C (Table 3 in their paper). Liu *et al.*[24] used simvastatin (T_g 31 °C) with lysine (T_g 68 °C) to form CAMS with T_g 29 °C.

The above examples further support the possibility of single-phase drug/AA CAMS with T_g close to that of the drug. This contradicts the Gordon–Taylor model, predicting that the T_g of a single-phase CAMS lies between the T_gs of the two components. By adopting AA values from Borredon *et al.*[36] (37.9 °C for LYS, 8.0 °C for MET and 10.9 °C for VAL), the expected T_gs of the developed CAMS are calculated as 63.0 °C for EXE/LYS 1 : 1, 54.3 °C for EXE/LYS 1 : 2, 21.4 °C for EXE/MET 1 : 1, and 42.1 °C for EXE/VAL 2 : 1 (Table S1). Since these values are very different from those in Fig. 7, the Gordon–Taylor model is not applicable, signifying that the assumptions of ideal mixing and linear temperature–volume dependence are not met for small molecules.[2]

Results of CAMS relaxation from isothermal microcalorimetry. Amorphous materials tend to gradually crystallize, with their molecular arrangement drifting toward the equilibrium supercooled melt.[23,25,38] In this journey, the system's internal energy and free volume both decrease while its structural order grows, a process referred to as structural relaxation[23,39] This process may continue beyond the timeframe of typical accelerated stability experiments. A number of studies have shown that following this relaxation in freshly made amorphous samples offers a practical window into their thermal history, thermodynamic behavior and stability.[23,40] In the present work, to quantify the degree of molecular activity and the rate of CAMS relaxation, the structural relaxation time (τ_D^β) was used. Low τ_D^β values correspond to high molecular mobility and fast relaxation.

Experimentally recorded relaxation curves of amorphous exemestane (aEXE) and CAMS of the drug with L-lysine (EXE/

LYS), L-methionine (EXE/MET) and L-valine (EXE/VAL) are shown in the SI (Fig. S2). Theoretical exponential decay relaxation curves computed using eqn (1) are superimposed on the experimental curves. Fitting eqn (1) to the experimental data is excellent (R^2 greater than 0.99037). Relaxation was quantified as the structural relaxation time (τ_D^β), which was computed using eqn (1) and (3) as explained in the experimental part. Values of parameters β and τ_D^β are listed in Table 4.

For the four CAMS, the τ_D^β values are 60.4203 for EXE/LYS 1 : 1, 77.2478 for EXE/LYS 1 : 2, 43.8475 for EXE/MET 1 : 1 and 13.5792 for EXE/VAL 2 : 1. The amorphous drug form (aEXE) has a τ_D^β of 20.4117. The higher τ_D^β of CAMS EXE/LYS 1 : 1, EXE/LYS 1 : 2 and EXE/MET 1 : 1 compared to aEXE confirm the stabilizing role of AAs as co-formers in the CAMS. They decrease molecular mobility and thus enhance the physical stability of the drug's amorphous form. On the other hand, EXE/VAL 2 : 1 CAMS showed a τ_D^β value lower than that of aEXE, indicating that VAL did not stabilize the amorphous drug, and hence, although there is coformability at a 2 : 1 molar ratio, physical stability appears to be problematic.

Table 4 Values of parameters β and τ_D^β in eqn (3) for the four CAMS and for the amorphous drug (aEXE)

CAMS	B	τ_D^β	R^2
aEXE	0.55 ± 0.000647	20.41	0.9884
EXE/LYS 1 : 1	0.49 ± 0.000745	60.42	0.9961
EXE/LYS 1 : 2	0.58 ± 0.000122	77.25	0.9918
EXE/MET 1 : 1	0.59 ± 0.001058	43.85	0.9904
EXE/VAL 2 : 1	0.48 ± 0.000235	13.58	0.9910

Physical stability under accelerated conditions. In Fig. 8, pXRDs of EXE/LYS 1 : 1, EXE/LYS 1 : 2, EXE/MET 1 : 1 and EXE/VAL 2 : 1 CAMS taken at the beginning of the stability test and after 30 and 90 days of storage under accelerated conditions (40 °C and 75% RH) are presented. For the equimolar EXE/LYS and EXE/MET and the EXE/LYS 1 : 2 CAMS, no re-crystallization peaks appeared at any time point (Fig. 8a–c). Therefore, despite the absence of drug–AA chemical interactions, as indicated by the FTIR spectra (Fig. 6), stable CAMS could be formed by sheer molecular mixing. This agrees with previously published results.[41–43]

Conversely, EXE/VAL 2 : 1 CAMS showed poor physical stability, with recrystallization peaks emerging after 90 days of

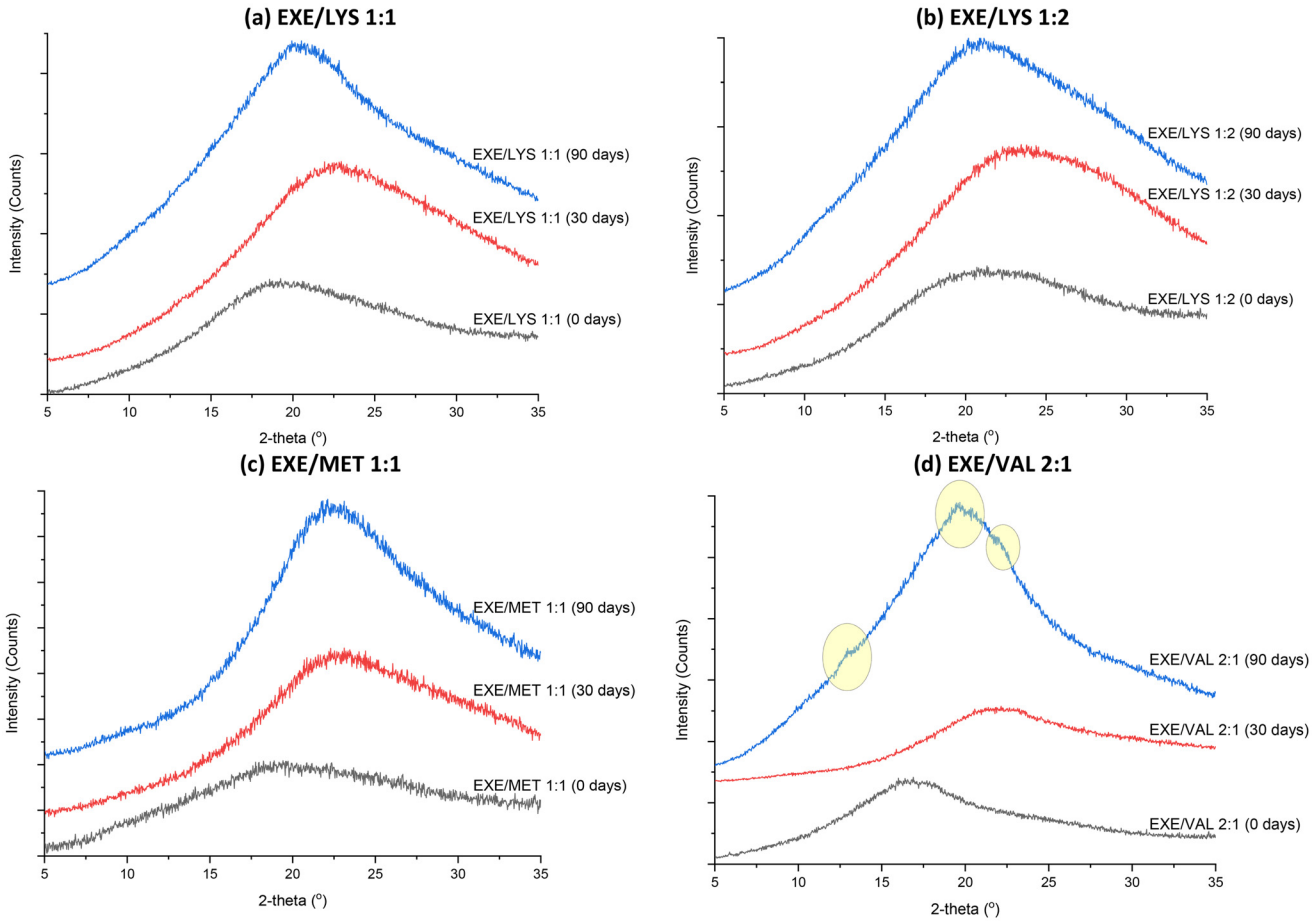

Fig. 8 pXRDs of CAMS of EXE/LYS at (a) 1 : 1 and (b) 1 : 2 molar ratios, (c) EXE/MET at a 1 : 1 molar ratio and (d) EXE/VAL at a 2 : 1 molar ratio at the beginning and after 30 and 90 days of the accelerated stability test at 40 °C and 75% RH.

storage (Fig. 8d). It is likely that the excess drug, whose molecular weight and weight proportion are much greater than those of the amino acid, renders the CAMS prone to disruption during the stability test. It is noticed that this recrystallization event tallies with the small relaxation time (τ_D^β) of 13.5792 h for EXE/VAL 2 : 1 CAMS (Fig. S2e), confirming the usefulness of τ_D^β as a proxy for CAMS physical stability.

Dissolution performance of the developed CAMS. Since the purpose of the CAMS is to increase drug solubility, dissolution and ultimately bioavailability, their *in vitro* performance is particularly important.

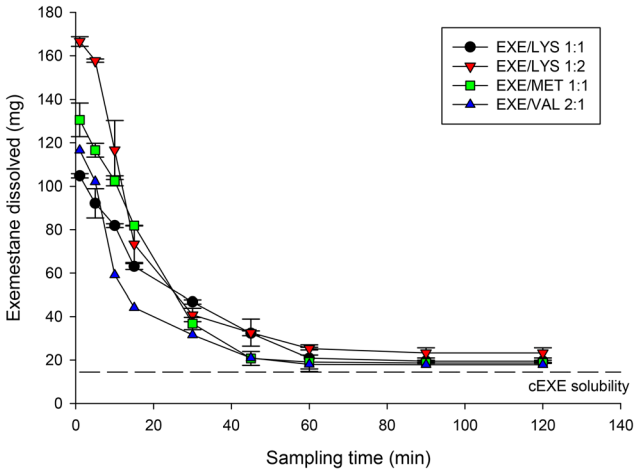

Fig. 9 Exemestane remaining dissolved *vs.* time profiles during the precipitation study of supersaturated solutions (solvent shift method for amorphous drug solubility). The dotted line corresponds to the solubility of the crystalline drug (cEXE).

Influence of the presence of amino acids on exemestane precipitation from solution. Fig. 9 shows profiles of EXE remaining dissolved over time after the addition of concentrated drug solution in DMSO to large volumes of aqueous AA solutions. This method is known as the Solvent Shift Method and estimates how effectively the amino acids engage with EXE in water, in other words, their ability to prevent precipitation under supersaturation conditions.[29,44] The sharp decline of dissolved EXE in the first 10–20 min (Fig. 9) reflects its transfer from the DMSO, where it is highly soluble into water, where it is poorly soluble. After this drop, the concentration of EXE and the supersaturation level remain constant for the remaining two hours of the test period, close to and slightly above the cEXE solubility. The EXE/LYS 2 : 1 CAMS seems to perform slightly better than the other CAMS. It can be concluded that the dissolved AAs slightly elevate the supersaturation levels over that of cEXE. This is not however expected to contribute significantly towards the dissolution improvement of the drug compared to the improvement due to the drug's association with the amino acids in the CAMS.[13,14]

In vitro dissolution performance under non-sink conditions. In Fig. 10, *in vitro* drug release profiles up to 24 h are presented for the developed EXE/LYS 1 : 1, EXE/LYS 2 : 1, EXE/MET 1 : 1, and EXE/VAL 2 : 1 CAMS. Since the release of the amorphous drug is expected to be higher than that of a crystalline drug, the experiments were performed under non-sink conditions (SI = 0.0116). For reference, release data for quench-cooled amorphous EXE (aEXE) and unprocessed crys-

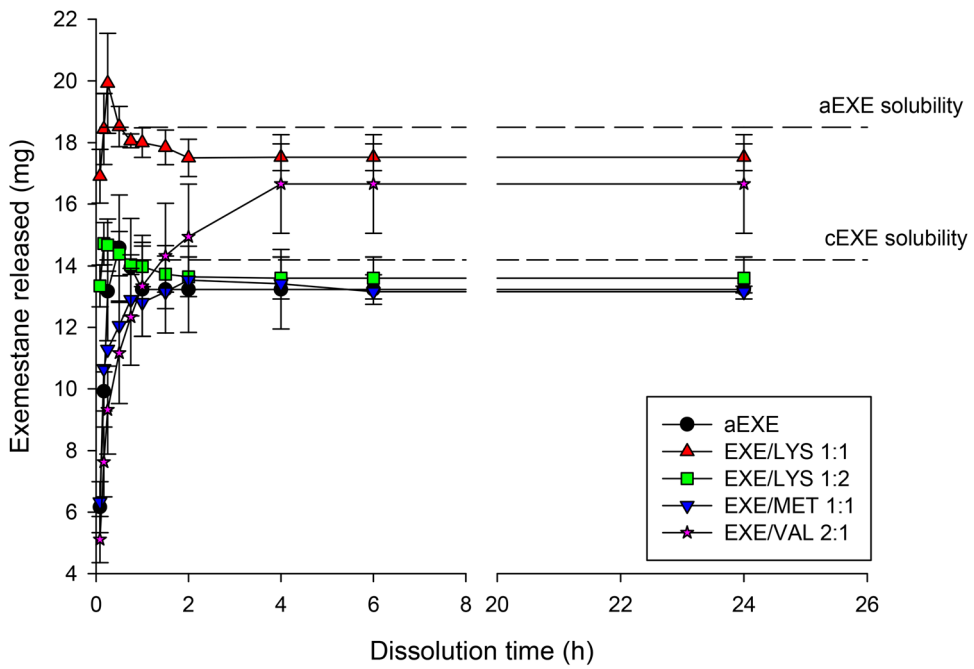

Fig. 10 Dissolution profiles of the test samples of exemestane from EXE/AA CAMS prepared by mHME and of the amorphous drug test sample (aEXE) prepared by quench cooling. Dashed lines correspond to the solubilities of the crystalline (cEXE) and amorphous drugs (aEXE).

talline EXE (cEXE) test samples are shown. Dotted lines indicate the equilibrium solubilities of aEXE and cEXE.

The aEXE alone test sample reaches a plateau close to the crystalline solubility, suggesting rapid recrystallisation when in contact with water. This is demonstrated by the pXRD profiles shown in Fig. S3 (SI) for solids remaining in the vessel at the end of the dissolution test of the developed CAMS EXE/LYS 1 : 1, EXE/LYS 1 : 2, EXE/MET 1 : 1 and EXE/VAL 2 : 1. The pXRD pattern of the recrystallized amorphous drug in the test sample is also shown. The release levels appear to be dependent on the amino acid and the EXE/AA molar ratio. EXE/LYS 1 : 1 delivers the strongest boost. For most of the experimental time, the dissolved concentration remains above the cEXE solubility and, during the first 15 min, even exceeds the aEXE solubility, producing a clear "spring–parachute" profile. It should be noted that the excess solid in the test sample that was used to maintain non-sink conditions remained amorphous throughout, whereas the sample of amorphous drug (aEXE) quickly recrystallized as seen in Fig. S3. The superior performance of EXE/LYS 1 : 1 is consistent with its lower $\Delta\delta_t$ and better miscibility compared with the EXE/MET and EXE/VAL systems (Table 3). The EXE/VAL 2 : 1 CAMS also showed high release levels that were sustained and formed a plateau well above the solubility of cEXE. The release profile is "rise to maximum" instead of "spring–parachute" seen for EXE/LYS 1 : 1, which implies low wettability of EXE in this CAMS, resulting in kinetic dissolution delay and masking of the 'spring and parachute effect'.[14] However, VAL is not a preferable conformer due to the poor physical stability of EXE/VAL 2 : 1 CAMS as was discussed previously.

In contrast, EXE/LYS 1 : 2, and EXE/MET 1 : 1 CAMS did not significantly improve the dissolution profile of EXE, showing similar profiles to that of the aEXE test sample. This behavior has been previously observed for 1 : 2 molar griseofulvin/lysine CAMS and has been attributed to extensive re-crystallization.[14] This is demonstrated clearly in Fig. S4 by the pXRD pattern of the remaining EXE/LYS 1 : 2 solids at the end of the dissolution test, showing distinct recrystallization peaks. Also, no dissolution improvement compared to the aEXE amorphous sample is seen in Fig. 10 for EXE/MET 1 : 1 CAMS, although there were no recrystallization events during dissolution (Fig. S3). In this case, the poor dissolution may be attributed to the hydrophobicity of MET, the highest among the three AAs studied.[14]

Conclusions

Feed solvent pretreatment hot-melt extrusion (mHME) enabled effective preparation of co-amorphous exemestane/amino acid systems at controlled extrusion temperatures that enabled processing without drug decomposition. Among the three amino acid (AA) co-formers of increasing hydrophobicity studied – L-lysine (LYS), L-valine (VAL) and L-methionine (MET) – L-lysine consistently produced fully amorphous EXE/LYS systems at 1 : 1 and 1 : 2 molar ratios, delivering superior physical stability (no recrystallization after 90 days at 40 °C/75% RH) and marked dissolution improvement under non-sink conditions. L-methionine co-amorphized only at an equimolar ratio and imparted moderate stabilization but no dissolution improvement, whereas L-valine coamorphized at a 2 : 1 ratio and yielded CAMS with limited shelf life but improved dissolution. These findings highlight the critical impact of co-former selection on the performance of co-amorphous formulations. Although there may be coformability, physical stability and release may be unsatisfactory. Considered together with the results of previous studies of our group, the mHME approach proved to be a robust, scalable strategy for producing stable CAMS of poorly soluble drugs with amino acids that demonstrated improved dissolution performance compared to the crystalline drug. Modern predictive software and specialized instrumentation could be used to provide more insight into drug–AA interactions at the molecular level and enlighten the formation, stability and dissolution performance of CAMS.

Author contributions

Ioannis Partheniadis: writing – original draft, methodology, investigation, funding acquisition, formal analysis, data curation, and conceptualization. Maria Tsouka: investigation. Ioannis Nikolakakis: writing – review & editing, methodology, investigation, funding acquisition, formal analysis, data curation, and conceptualization.

Conflicts of interest

The authors declare that they have no known competing financial interests or personal relationships that could have appeared to influence the work reported in this paper.

Data availability

The authors confirm that the data supporting the findings of this study are available within the article. Additional data that support the findings of this study are available on the Open Science Framework (OSF) Repository: https://osf.io/qbrsu/.

Supplementary information: DSC, pXRD, ATR-FTIR raw data, and HPLC calibration curves. See DOI: https://doi.org/10.1039/d5pm00146c.

Acknowledgements

This research work was supported by the Hellenic Foundation for Research and Innovation (HFRI) under the 4th Call for HFRI PhD Fellowships (Fellowship Number: 9335). Ioannis Partheniadis gratefully acknowledges the Department of Pharmacy at the University of Copenhagen for hosting him as a visiting PhD researcher under the Erasmus+ Traineeship Program Student Mobility. The authors express their gratitude

to Associate Professor Dr Inês C. B. Martins and Research Chair Professor Dr Thomas Rades at the Department of Pharmacy, University of Copenhagen, for generously providing access to the TAM and DMA instruments. Additionally, the authors extend their appreciation to Associate Professor Dr Panagiotis Barmpalexis and Dr Afroditi Kapourani of the Laboratory of Pharmaceutical Technology at the School of Pharmacy of the Aristotle University of Thessaloniki for their kind support in facilitating pXRD measurements.

References

1 A. Karagianni, K. Kachrimanis and I. Nikolakakis, *Pharmaceutics*, 2018, **10**, 98.
2 J. Liu, H. Grohganz, K. Löbmann, T. Rades and N. J. Hempel, *Pharmaceutics*, 2021, **13**, 389.
3 S. Narala, D. Nyavanandi, P. Srinivasan, P. Mandati, S. Bandari and M. A. Repka, *J. Drug Delivery Sci. Technol.*, 2021, **61**, 102209.
4 I. Nikolakakis and I. Partheniadis, *Pharmaceutics*, 2017, **9**, 50.
5 S. J. Dengale, H. Grohganz, T. Rades and K. Löbmann, *Adv. Drug Delivery Rev.*, 2016, **100**, 116–125.
6 E. Lenz, K. Löbmann, T. Rades, K. Knop and P. Kleinebudde, *J. Pharm. Sci.*, 2017, **106**, 302–312.
7 A. T. Heikkinen, L. DeClerck, K. Löbmann, H. Grohganz, T. Rades and R. Laitinen, *Pharmazie*, 2015, **70**, 452–457.
8 K. T. Jensen, F. H. Larsen, C. Cornett, K. Löbmann, H. Grohganz and T. Rades, *Mol. Pharm.*, 2015, **12**, 2484–2492.
9 K. T. Jensen, K. Löbmann, T. Rades and H. Grohganz, *Pharmaceutics*, 2014, **6**, 416–435.
10 K. Kachrimanis and I. Nikolakakis, in *Handbook of Polymers for Pharmaceutical Technologies*, ed. V. K. Thakur and M. K. Thakur, 2015, pp. 121–149.
11 I. Partheniadis, M. Toskas, F.-M. Stavras, G. Menexes and I. Nikolakakis, *Processes*, 2020, **8**, 1208.
12 J. Wesholowski, K. Hoppe, K. Nickel, C. Muehlenfeld and M. Thommes, *Eur. J. Pharm. Biopharm.*, 2019, **142**, 396–404.
13 I. Partheniadis and I. Nikolakakis, *Int. J. Pharm.*, 2024, **652**, 123824.
14 I. Partheniadis, M. Tsouka and I. Nikolakakis, *Int. J. Pharm.*, 2024, **666**, 124818.
15 M. T. França, T. M. Marcos, R. N. Pereira and H. K. Stulzer, *Eur. J. Pharm. Sci.*, 2020, **143**, 105178.
16 J. A. Baird, B. Van Eerdenbrugh and L. S. Taylor, *J. Pharm. Sci.*, 2010, **99**, 3787–3806.
17 ASTM E2550-17 https://store.astm.org/e2550-17.html.
18 X. Chen, I. Partheniadis, I. Nikolakakis and H. Al-Obaidi, *Polymers*, 2020, **12**, 854.
19 A. Forster, J. Hempenstall, I. Tucker and T. Rades, *Int. J. Pharm.*, 2001, **226**, 147–161.
20 D. J. Greenhalgh, A. C. Williams, P. Timmins and P. York, *J. Pharm. Sci.*, 1999, **88**, 1182–1190.
21 E. Stefanis and C. Panayiotou, *Int. J. Thermophys.*, 2008, **29**, 568–585.
22 B. Konda, R. N. Tiwari and H. Fegade, *J. Chromatogr. Sci.*, 2011, **49**, 634–639.
23 C. Bhugra, R. Shmeis, S. L. Krill and M. J. Pikal, *J. Pharm. Sci.*, 2008, **97**, 455–472.
24 J. Liu, D. R. Rigsbee, C. Stotz and M. J. Pikal, *J. Pharm. Sci.*, 2002, **91**, 1853–1862.
25 I. C. B. Martins, A. S. Larsen, A. Madsen, O. A. Frederiksen, A. Correia, K. Jensen, H. S. Jeppesen and T. Rades, *Chem. Sci.*, 2023, **14**, 11447–11455.
26 A. Kapourani, A. T. Chatzitaki, I. S. Vizirianakis, D. G. Fatouros and P. Barmpalexis, *Int. J. Pharm.*, 2023, **640**, 123004.
27 N. S. Trasi and L. S. Taylor, *J. Pharm. Sci.*, 2015, **104**, 2583–2593.
28 K. Ueda, S. S. Hate and L. S. Taylor, *J. Pharm. Sci.*, 2020, **109**, 2464–2473.
29 T. Yamashita, S. Ozaki and I. Kushida, *Int. J. Pharm.*, 2011, **419**, 170–174.
30 A. Singh, Y. R. Neupane, B. Mangla and K. Kohli, *J. Pharm. Sci.*, 2019, **108**, 3382–3395.
31 G. Kasten, K. Nouri, H. Grohganz, T. Rades and K. Löbmann, *Int. J. Pharm.*, 2017, **533**, 138–144.
32 G. Kasten, K. Löbmann, H. Grohganz and T. Rades, *Int. J. Pharm.*, 2019, **557**, 366–373.
33 J. J. Jayapal and S. Dhanaraj, *Int. J. Biol. Macromol.*, 2017, **105**, 416–421.
34 M. B. Mary, V. Sasirekha and V. Ramakrishnan, *Spectrochim. Acta, Part A*, 2006, **65**, 955–963.
35 B. R. Adhikari, S. Sinha, K. C. Gordon and S. C. Das, *Int. J. Pharm.*, 2022, **621**, 121799.
36 C. Borredon, L. A. Miccio, S. Cerveny and G. A. Schwartz, *J. Non-Cryst. Solids:X*, 2023, **18**, 100185.
37 B. R. Adhikari, S. Sinha, N. Lyons, D. Pletzer, I. Lamont, K. C. Gordon and S. C. Das, *Eur. J. Pharm. Biopharm.*, 2022, **180**, 260–268.
38 S. L. Shamblin, B. C. Hancock and M. J. Pikal, *Pharm. Res.*, 2006, **23**, 2254–2268.
39 K. Kawakami and Y. Ida, *Pharm. Res.*, 2003, **20**, 1430–1436.
40 A. M. Abdul-Fattah, K. M. Dellerman, R. H. Bogner and M. J. Pikal, *J. Pharm. Sci.*, 2007, **96**, 1237–1250.
41 S. J. Dengale, O. P. Ranjan, S. S. Hussen, B. S. M. Krishna, P. B. Musmade, G. Gautham Shenoy and K. Bhat, *Eur. J. Pharm. Sci.*, 2014, **62**, 57–64.
42 K. Löbmann, H. Grohganz, R. Laitinen, C. Strachan and T. Rades, *Eur. J. Pharm. Biopharm.*, 2013, **85**, 873–881.
43 K. Löbmann, R. Laitinen, C. Strachan, T. Rades and H. Grohganz, *Eur. J. Pharm. Biopharm.*, 2013, **85**, 882–888.
44 J. Bevernage, J. Brouwers, M. E. Brewster and P. Augustijns, *Int. J. Pharm.*, 2013, **453**, 25–35.